JRC Scientific and Technical Reports

Constraint-Based Master Curve Analysis of a Nuclear Reactor Pressure Vessel Steel

results from an experimental programme carried out within the IAEA CRP-8 project

Philip Minnebo, César Chenel Ramos, José Mendes, Luigi Debarberis

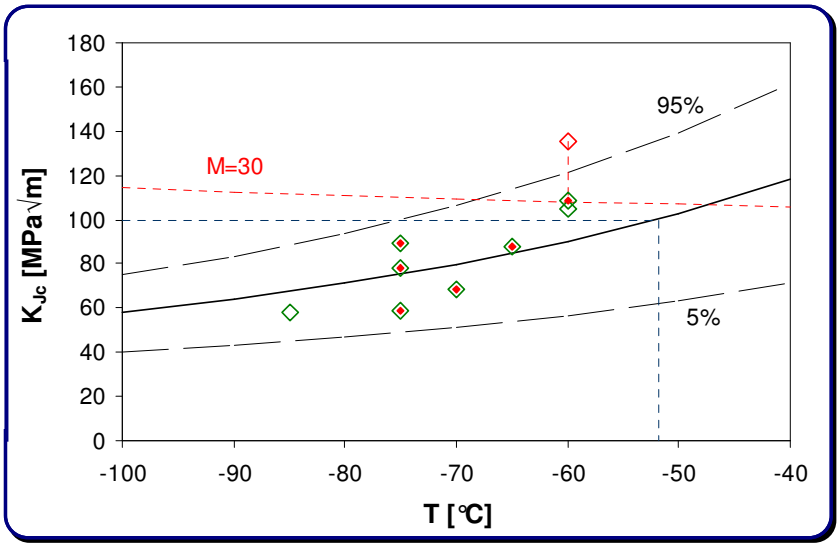

EUR 24092 EN - 2009

JRC EUROPEAN COMMISSION

Institute for Energy

The mission of the JRC-IE is to provide support to Community policies related to both nuclear and non-nuclear energy in order to ensure sustainable, secure and efficient energy production, distribution and use.

European Commission
Joint Research Centre
Institute for Energy

Contact information

Address: Philip Minnebo, P.O. Box 2, 1755ZG Petten, The Netherlands
E-mail: philip.minnebo@jrc.nl
Tel.: +31 224 565461
Fax: +31 224 565641

http://ie.jrc.ec.europa.eu
http://www.jrc.ec.europa.eu

JRC55263
EUR 24092 EN

Printed in The Netherlands

ABSTRACT

This report presents the outcome of four fracture test series, addressing the ductile-to-brittle toughness behaviour of a nuclear reactor pressure vessel steel. Each test series corresponds to a specific test specimen geometry, tensile or three-point-bend, with a given degree of crack-tip constraint. A brief overview is given of available constraint-based fracture mechanics methodologies in the ductile-to-brittle transition range, including both engineering and local approach procedures. The obtained experimental data are analysed by means of the Master Curve standard ASTM E1921. Variability of the resulting reference temperature, T_0, is successfully confirmed by a selection of constraint-based methodologies.

CONTENTS

1. INTRODUCTION

The Institute for Energy (IE) was intensively involved in the Eighth Co-ordinated Research Project (CRP-8) of the International Atomic Energy Agency (IAEA). This project, which ran from 2004 until 2007, focused on the Master Curve (MC) methodology, which is frequently applied for characterizing fracture toughness of ageing nuclear Reactor Pressure Vessels (RPVs) in the ductile-to-brittle transition region. Within the CRP, three topic areas were considered to require further study and consensus: influence of crack-tip constraint, effect of loading rate and general validity of the MC shape.

The topic area dedicated to crack-tip constraint focused on the influence of test specimen bias and geometry on the MC reference temperature (T_0). In this context the IE performed and analysed four test series with different types of laboratory specimens, each of them corresponding to a certain degree of constraint. In addition to this experimental programme, the IE also participated in an analytical round robin task aiming at validation of finite element tools needed to assess the loss of crack-tip constraint in shallow crack bend specimens.

This report presents the analysis of the four test series mentioned above. Before giving this analysis, the MC method is briefly presented as well as a selection of related constraint-based fracture mechanics approaches. The limited number of experiments carried out did of course not allow for a reliable validation of these methodologies. Nevertheless it was judged meaningful to check whether the available standard size data sets follow the trends predicted by some selected theories. In this context, the experimental data were also linked to the outcome of the finite element modelling exercise carried out by the IE within the same CRP topic area.

2. MASTER CURVE METHODOLOGY

The MC approach assumes that typical ferritic steels used for light-water RPVs show the same probabilistic ductile-to-brittle transition behaviour, which is indexed by only one single parameter: the MC reference temperature T_0. For the median K_{Jc} fracture toughness, corresponding to a 50% cumulative probability for cleavage failure, following temperature distribution is put forward in the MC standard ASTM E1921 [1]:

$$K_{Jc}^{med} = 30 + 70.e^{0.019(T-T_0)} \qquad \text{[MPa}\sqrt{\text{m}}\text{]} \qquad \text{(a)}$$

K_{Jc} is related to the J-integral at final fracture (J_c) through a plane-strain relationship, which includes Young's modulus E and Poison's ratio υ:

$$K_{Jc} = \sqrt{J_c \frac{E}{1-\upsilon^2}} \qquad \text{[MPa}\sqrt{\text{m}}\text{]} \qquad \text{(b)}$$

Equation (a) is based on weakest-link theory with accumulated failure probability described by a three-parameter Weibull distribution. Two of these parameters are assumed to be fixed for all ferritic RPV steels: the Weibull modulus m = 4 and the threshold toughness K_{min} = 20 MPa√m. The remaining variable parameter is the scale parameter K_0, which corresponds to a 63% cumulative probability level for failure by cleavage. [1] further describes the methods – which may only require as few as six fracture tests – to determine the reference temperature T_0. The latter corresponds to a median K_{Jc} value of 100 MPa√m. An aspect to be stressed is that the applied weakest-link approach implies that measured fracture toughness depends on crack front length (or specimen thickness). Actually, expression (a) describes the behaviour of 25 mm thick test specimens. K_{Jc} toughness measured with specimens of different thickness B is to be converted as follows before completing the T_0 analysis:

$$K_{Jc}^{25mm} = K_{\min} + (K_{Jc} - K_{\min}).\left(\frac{B}{25mm}\right)^{\frac{1}{4}} \qquad \text{[MPa√m]} \qquad \text{(c)}$$

The MC description of the ductile-to-brittle transition behaviour of typical RPV steels has been validated through numerous projects, using large amounts of available K_{Jc} fracture toughness data. Figure 1 shows an example taken from the NESC-IV project, which addressed ASTM A533 grade base and weld metal. In addition to the median, the 1%, 5%, 95% and 99 % probability bounds are given for a longitudinal RPV weld [2]. T_0 was found to be -94.8 °C. Conventional application of the MC concept assumes that material degradation can be quantified through a simple shift of T_0 towards higher temperature with conservation of the MC shape. In addition to this, various studies have been published, which treat phenomena such as crack-tip constraint loss and even biaxial loading conditions basically in an analogue way, i.e. by re-evaluation of T_0 (K_0) with unchanged m and K_{min} figures. Nevertheless, as also found during the CRP-8 project, further investigations are still required in these areas.

In spite of the development of the MC method, which has proven to be an excellent tool for probabilistic safety assessment, the regulatory approaches to ageing RPV integrity assessment are still heavily based on impact experimental data. US Nuclear Regulatory Commission (NRC) legislation uses the "traditional" RT_{NDT} reference temperature, which is calculated from Pellini drop weight and Charpy impact tests performed on unirradiated material. This reference temperature is used in the ASME Boiler and Pressure Vessel Code [3] to index two lower bound fracture toughness curves, i.e. initiation toughness and dynamic/arrest toughness. The former is defined as follows:

$$K_{Ic} = 36.48 + 22.783\, e^{0.036(T - RT_{NDT})} \qquad \text{[MPa√m]} \qquad \text{(d)}$$

Material ageing from irradiation is measured as the shift of the Charpy energy transition curve at the 41 J level. The ASME lower bound curves are shifted accordingly ($\Delta RT_{NDT} = \Delta T_{41J}$), assuming that this shift measured under dynamic

conditions also quantifies the RPV material ageing in terms of actual quasi-static fracture toughness. This and other deficiencies are taken into account by imposing conservative bounds on toughness estimates, potentially penalizing plant operation decisions. The variable degree of conservatism of this regulatory approach can be mitigated by direct measurement of the MC reference temperature T_0 (possible with a limited number of small specimens) and applying the procedures outlined in ASME Code Cases N-629 [4] and N-631 [5]. The latter allows the replacement of RT_{NDT} in the lower bound fracture curve by the equivalent RT_{T0}, which is deduced from the "directly" measured T_0 by means of following empirical formula: $RT_{T0} = T_0 + 19.4$ °C. The effect of this procedure is shown in Figure 2, which also originates from the NESC-IV report [2] and gives the ASME curves based both on RT_{NDT} and RT_{T0} for the same weld metal that was presented in Figure 1. From Figure 2 it is also obvious that the ASME RT_{T0}-based curve is quite close to the MC 1% lower bound line.

3. CONSTRAINT-BASED FRACTURE MECHANICS IN THE DUCTILE-TO-BRITTLE TRANSITION RANGE

3.1. Macroscopic concepts

Conventional "macroscopic" or "global" fracture mechanics approaches, including those applicable in the ductile-to-brittle transition range of ferritic RPV steels, assume that the state of stress and strain nearby a crack tip can be characterised by one single parameter. Under predominantly elastic conditions this parameter is the stress intensity factor K_{Ic}. In case of more widespread yielding the *J*-integral or the *Crack Tip Opening Displacement* (*CTOD*) concepts can be used. The single parameter controlled crack-tip fields must encompass the region in which the fracture process takes place. The extent of these fields depends on the geometry, size and loading mode of the structure or specimen containing the crack. In standard fracture mechanics testing of metals, deep crack specimens with minimum dimensional requirements are prescribed to ensure "valid" results. These requirements provide a high degree of crack-tip constraint, which corresponds to near plain strain, Small Scale Yielding (SSY) conditions. Fracture toughness measured under these circumstances can be used as lower bound data for a given material and temperature. However real defective structures (e.g. containing sub-surface shallow cracks) may provide more elevated values of toughness when compared with "valid" laboratory results. This elevation of toughness occurs because such geometries impose a relatively low level of crack-tip constraint. In order to quantify this decay of constraint, a second factor has to be used besides the conventional fracture toughness parameter (e.g. *J*), as the latter on its own is unable to assess how the structural and loading configuration affects the constraint conditions at the crack tip.

Various two-parameter approaches are available in conjunction with the *K* and *J* fracture toughness concepts. These include the mathematically rigorous K-T_{stress} and J-A_2 methods, which increase the area of dominance of the asymptotic *K* or *J* fields, and the phenomenological *J-Q* and *J-h* concepts. In all cases, the degree of

constraint can be described in a unique manner in terms of the secondary fracture parameter. The most popular parameters used for the description of crack-tip constraint conditions in the ductile-to-brittle range are T_{stress} and Q. A good basic description of these concepts can be found in [6]. In current report only the K-T_{stress} approach is briefly presented as the Q parameter, which is able to account for larger-scale plasticity and evaluate the effect of "out-of-plane" conditions, requires detailed finite element modelling, which is outside the scope of this paper.

The K-T_{stress} concept considers both the first (singular) and second (non-singular) term of the Williams extension of the plane strain crack front stress field (in terms of the polar co-ordinates r and φ):

$$\sigma_{ij}(r,\varphi) = \frac{K_I}{(2\pi)^{\frac{1}{2}}} r^{-\frac{1}{2}} f_{ij}^{(1)}(\varphi) + T_{stress} r^0 f_{ij}^{(2)}(\varphi) + \ldots \qquad \text{(e)}$$

$f_{ij}^{(n)}(\varphi)$ is a dimensionless circumferential stress distribution. T_{stress}, which scales with the applied load, can be assessed through a relatively straightforward elastic analysis. Moreover ready-for-use handbook solutions are available for common cracked geometries. The use of T_{stress} has been extensively promoted in connection with the MC approach. In the case of Single Edge Notched Bend – SEN(B) – bars, it has been empirically shown that for small or positive T_{stress} values the measured fracture toughness remains practically constant. This observation is connected to the presence of high crack-tip constraint conditions. In case of constraint loss – i.e. in shallow flaw SEN(B) specimens – T_{stress} becomes increasingly more negative and measured fracture toughness starts to rise rapidly. Herewith it is assumed that the MC shape "is not significantly affected" (see also previous paragraph). A simple conservative relation between T_{0deep} obtained from deeply cracked (high constraint) SEN(B) bars and T_0 linked to shallow crack specimens (low constraint conditions) is proposed and checked in [7]:

$$T_0 \approx T_{0deep} + \frac{T_{stress}}{10MPa/°C} \; for \; T_{stress}\,[MPa] < 0 \qquad \text{(f)}$$

This equation is based on the assumption that test specimen failure always occurs close to the plastic limit load. Alternatively, paper [8] suggests following more complex relation between T_{stress} [MPa] and the connected T_0 shift (σ_y is the material's yield strength in MPa):

$$\Delta T_0 = -50.6\left(\frac{T_{stress}}{\sigma_y}\right)^3 - 118.4\left(\frac{T_{stress}}{\sigma_y}\right)^2 - 15.1\left(\frac{T_{stress}}{\sigma_y}\right) - 0.513 \qquad \text{(g)}$$

As is the case for equation (f), the use of relationship (g) is limited to the estimation of the T_0 shift related to test specimens showing negative T_{stress} values. More recent research has revealed significant difference between T_0 estimates arising from

deeply notched SEN(B) bars and Compact Tension – C(T) – specimens, both of which show a positive T_{stress}. The following equation, which has been presented in [9], anticipates to this finding and allows for comparison of specimens showing positive T_{stress}:

$$\Delta T_0 \approx \frac{T_{stress}}{12MPa/°C} \; for \; T_{stress} < 300MPa \tag{h}$$

3.2. Local approaches

Local approach concepts are based on the local mechanical stress and strain fields in the fracture process zone ahead of the crack front. Considering the scope of this paper, which is related to cleavage fracture in the ductile-to-brittle transition range, the Weibull stress or Beremin micromechanical model is highlighted here [10]. The finite element round robin exercise organised within the CRP-8 selected this approach for the assessment of crack-tip constraint in laboratory fracture bend bars. It allows quantifying the evolution of 3-D crack-front fields as SSY conditions decay under increased loading. The model uses the Weibull stress σ_w as local fracture parameter and defines the global cumulative probability for cleavage fracture as follows:

$$P_f(\sigma_w) = 1 - e^{\left[-\left(\frac{\sigma_w}{\sigma_u}\right)^m\right]} \tag{i}$$

Herein the scalar Weibull stress is given by:

$$\sigma_w = \left[\frac{1}{V_0}\int_V \sigma_1 \, dV\right]^{\frac{1}{m}} \tag{j}$$

The Weibull stress is thus computed by integrating the maximum principal stress σ_1 over the fracture process zone V, which is commonly defined as the volume where $\sigma_1 \geq 2.\sigma_0$. V_0 is an arbitrary reference volume. The Weibull modulus m quantifies the degree of scatter in the cumulative failure probability distribution. The scale parameter σ_u is the Weibull stress value for which P_f = 0.63. The two-parameter (m, σ_u) model given above can be extended to a three-parameter concept, introducing σ_{min}, which corresponds to the threshold toughness for the given material.

Estimation of m and σ_u requires availability of fracture data covering two distinct constraint levels. High constraint data are usually obtained from testing deep crack fracture specimens, whereas low constraint data typically arise from shallow flaw bend bars. Further to this, detailed elastic-plastic finite element analysis of both

specimen geometries must be performed, resulting in accurate figures for the Weibull stress σ_w and the connected J (K_J) levels. The same parameters must be evaluated for a crack in an infinite body under plane strain, SSY conditions. Figure 3 gives a schematic, which shows the typical difference between the σ_w - J relations obtained for the SSY situation and the two selected constraint levels. Calibration of m basically consists of an iterative procedure that minimises the difference between the SSY scale factors for the J_c distribution, which are linked to the two selected crack-tip constraint levels. σ_u is the σ_w value resulting from the SSY analysis with the optimised scale factor used as input crack driving force [9].

The Weibull stress model can be linked to the ASTM E1921 procedure in order to more accurately describe constraint loss effects on measured fracture toughness relative to the plane strain, SSY reference condition.

3.3. Treatment of crack-tip constraint in the ASTM E1921 standard

[1] allows the use of following fracture specimen geometries: C(T), SEN(B) and Disk-shaped Compact Tension (DC(T)). A range of specimen sizes with proportional dimensions is recommended. For bend bars, specimen width (W) may be once or twice specimen thickness (B). For all cases the pre-fatigued initial crack length (a_0) is required to be in between 0.45W and 0.55W. The use of deeply cracked specimens is a major requirement towards sufficiently high constraint conditions. The application of side grooves, which are optional, is helpful to assure pre-test crack front straightness and, at the same time, also counteracts (out-of-plane) constraint loss near the edges of the specimen. This may be particularly important in case of low-thickness fracture bars, where near plane stress conditions may occur. In addition to this, a number of rather general statements are made in [1] regarding the crack-tip constraint issue. Within the "Scope" of the standard, for example, it is mentioned that median K_{Jc} levels at a certain temperature tend to vary with specimen type, “presumably due to constraint differences”. The “best estimate” average difference observed between T_0 resulting from C(T) and SEN(B) specimens is reported to be 10 °C, with the C(T) configuration giving the highest figure.

Formally the requirement for sufficiently high crack-front constraint is expressed as follows for all allowed specimen types and sizes:

$$K_{Jc(\text{limit})} = \sqrt{\frac{Eb_0\sigma_y}{30\left(1-\upsilon^2\right)}} \qquad \text{[MPa}\sqrt{\text{m}}\text{]} \qquad \text{(k)}$$

This value defines the threshold K_{Jc} level, below which constraint is considered not to affect measured toughness. It is also obvious that the remaining ligament $b_0 = W - a_0$ is put forward as the only limiting dimensional factor with regard to the specimen’s measurement capacity. In addition, it must be stressed that K_{Jc} data exceeding the limit value can still be used for evaluation of T_0, by applying the censoring procedure as explained in the standard. On the other hand, the standard

suggests that in case of “small specimens” equation (k) may not be fully adequate, possibly resulting in non-censoring of specimens with considerable constraint loss and consequent non-conservative estimation of T_0.

This problem primarily relates to the use of 10x10 mm Charpy-size bars, which are predominant in surveillance capsule programmes. The central issue is thus the value to be adopted for the so-called *M*-factor (that is set equal to 30 in above equation) in order to maintain sufficiently high constraint conditions in individual fracture specimens, e.g. corresponding to maximum 20% constraint loss with respect to SSY predictions. Numerical analyses have shown that this *M*-factor value depends on specimen type and material properties, such as yield stress and strain hardening exponent. A study reported in paper [11], which also summarizes many findings from previous research, concludes that M = 30-50 is sufficient to avoid constraint effects in a C(T) specimen geometry. For bend specimens however, censoring with M = 150-300 is required to obtain constraint-insensitive T_0 values. This applies to both *B*x*B* and *B*x2*B* standard type bars. For small 10x10 mm bars however this approach normally results in a drastic reduction of the allowable test temperature range, making it almost impossible to determine a valid T_0 in accordance with the standard procedure. As a “short-term remedy” [11] proposes to employ a (slightly conservative) 15 °C upward shift of T_0 for bend bars with insufficient M values, although it would be more desirable to use methods for the adjustment of individual K_{Jc} values to eliminate specimen geometry bias.

In article [12] a fully experimental quantitative constraint correction is given, which is based on a distribution comparison technique, involving 12.5 mm C(T) and 10x10 mm SEN(B) fracture toughness data. The C(T) specimen, corrected for the statistical size effect, is taken to represent the SSY value for the SEN(B) bar. The results were described by following decaying exponential function:

$$\frac{J_{SEN(B)10x10}}{J_{SSY\,C(T)}} = 1.35\left[1 + 1.5\,e^{(-M/10)}\right] \qquad \text{(l)}$$

Alternatively, paper [13] presents two separate equations to adjust the T_0 obtained from SEN(B) bars to that corresponding to a 25 mm C(T) specimen geometry (SSY):

$$\frac{K_{Jc\ SEN(B)}}{K_{Jc\ C(T)}} = 1.10 + 0.00053\left[175 - M\right] \quad \text{for SEN(B) Bx2B} \qquad \text{(m)}$$

$$\frac{K_{Jc\ SEN(B)}}{K_{Jc\ C(T)}} = 1.19 + 0.00180\left[120 - M\right] \quad \text{for SEN(B) BxB} \qquad \text{(n)}$$

4. CRP-8 EXPERIMENTAL PROGRAMME CARRIED OUT AT THE IE

4.1. Summary

In order to contribute to the experimental database required by the constraint-related CRP-8 topic area, four dedicated test series were carried out at the IE in accordance with ASTM standard E1921. These series involved four types of fracture mechanics specimens, each of them with an (at least potentially) different degree of crack-tip constraint (see above):

- C(T)10 mm (a_0/W~0.5)) – type A;
- SEN(B)10x20 mm (a_0/W~0.5) – type B;
- SEN(B)10x10 mm (a_0/W~0.5) – type C;
- SEN(B)10x10 mm (a_0/W~0.1) – type D.

As is also clear from Figure 4, the overall programme was designed as such that "subsequent" specimens only differed by one single characteristic parameter: loading geometry, specimen width or relative crack depth.

4.2. Test material

The JRQ “reference steel” was selected to carry out the experimental programme. This ASTM A533 grade B class 1 RPV steel served for many years as a radiation – mechanical property correlation monitor material in a number of national and international projects, studying irradiation embrittlement of RPV steel. “Extra” copper was added to the typical A533 chemical composition to ensure high sensitivity to neutron embrittlement, as is apparent from Table 1. The test specimens were machined from the so-called block “8JRQ44”, which originates from JRQ “plate B” [14]. Figure 5 shows a sampling plan related to one layer taken out of “8JRQ44”.

It should be noted that the JRQ steel in general was found to show significant through-wall inhomogeneity, both in terms of microstructure and mechanical and fracture properties [15]. RPV fracture toughness is usually higher towards the plate surfaces due to quenching rate effects. To exclude or at least minimise influence from material inhomogeneity, all fracture test specimens were taken out close to each other, 50 to 90 mm below the plate surface and all of them were oriented in the same direction (“TL”).

4.3. Method

In general, the experimental procedures laid down in ASTM E1921 were always followed for the fracture experiments. Properly maintained and calibrated equipment was used for the test programme. Specimens were cooled down in a temperature-controlled chamber, making use of liquid nitrogen.

Pre-cracking was performed under ΔK-controlled conditions, with the final $\Delta K \approx$ 12 MPa√m, assuring sharp fatigue cracks. The K_{min}/K_{max} ratio was always set equal to 0.1. In order to prepare the shallow-flaw 10x10 mm SEN(B) specimens (type D), 10 x 20 mm type B-like bend bars were pre-cracked and subsequently machined to the final dimensions, as is illustrated in Figure 6. Given the short crack length of nominally 1 mm, the resulting bars could not include integrated knife edges for *CMOD* (Crack Mouth Opening Displacement) measurement. Instead, external knife edges with thickness 1.7 mm were mounted for the actual fracture tests (see also below).

The plastic component of J at the onset of cleavage fracture (J_p) was always calculated starting from the load (P) – *CMOD* records. In case of the shallow-flaw bars, which did not contain integrated knifes, the clip gauge displacement $CMOD_z$ recorded at the external knife edges (at distance z from the specimen surface) was corrected to the equivalent *CMOD* at the surface [16]:

$$CMOD = CMOD_z \frac{a_0 + r_p(W - a_0)}{a_0 + r_p(W - a_0) + z} \qquad \text{[mm]}; \quad z = 1.7 \text{ mm} \qquad \text{(o)}$$

The plastic rotation factor r_p was obtained from:

$$r_p = 0.3 + 0.5\frac{a_0}{W} \qquad \text{[mm]} \qquad \text{(p)}$$

The subsequent step, i.e. linking J_p to the "plastic" area under the P – *CMOD* trace (A_p) requires a plastic èta-factor (η), which is given in ASTM E1921 for all specimen types, except for the non-standard shallow-flaw bend bars. For the latter, following formula was adopted within the CRP-8 consortium [16]:

$$\eta = 3.785 - 3.101\left(\frac{a_0}{W}\right) + 2.018\left(\frac{a_0}{W}\right)^2 \qquad \text{(q)}$$

This equation assumes that the span of the three-point test set-up is equal to four times the bend specimen width.

Subsequently the total *J-integral* at the onset of cleavage was calculated as follows:

$$J_c = J_p + \frac{(1 - \upsilon^2) K_e^2}{E} \qquad \text{[MN/m]} \qquad \text{(r)}$$

with K_e an elastic stress intensity factor based on the specific specimen geometry and dimensions and the measured load at fracture.

Finally K_{Jc} [MPa√m] was evaluated by means of equation (b).

4.4. Supporting tensile data

Young's modulus (E) is needed to evaluate J_c and K_{Jc} (see previous paragraph). Within the reported analyses, E is always calculated from following formula, which has proven to be accurate for ferritic steel grades in the addressed temperature range [17]:

$$E = 207200 - 57.1\,T\,(°C) \qquad \text{[MPa]} \qquad \text{(s)}$$

0.2% proof stress ($R_{p0.2}$) is included in the assessment of $K_{Jc(limit)}$. It was decided to carry out a number of dedicated tension tests, fully in accordance with ASTM E8-04 [18], in order to dispose of specific data for the given sampling area in block "8JRQ44". The resulting engineering tensile curves obtained at room temperature, -25 °C and -70 °C are presented in Figure 7. The corresponding $R_{p0.2}$ – temperature data points were compared with the trend given in [16] for JRQ steel in general. As the correspondence was quite good, it was decided to further use the equation from [16]:

$$R_{p0.2} = 4.10^{-8}\,T^4 - 2.10^{-5}\,T^3 + 3.6\,.10^{-3}\,T^2 - 0.543T + 490 \qquad \text{(t)}$$

Herein T is expressed in °C and $R_{p0.2}$ in MPa.

4.5. Analysis strictly following the ASTM E1921-05 procedure

For each test series, the K_{Jc} – test temperature data calculated by means of the method presented in paragraph 4.2. were analysed strictly in accordance with the ASTM E1921-05 multi-temperature analysis procedure. This implies the use of an M-factor value equal to 30 for all sets, including the ones using the Charpy-sized deep and shallow crack bend bars. Table 2 gives the resulting T_0 values as well as the two following properties, which are defined in [1]:

- $\Sigma\, r_i\, n_i$, with r_i the number of valid tests within a given temperature range (with respect to T_0) and n_i the weighting factor corresponding to that range. A $\Sigma\, r_i\, n_i$ value of at least 1 is required for a valid determination of T_0.
- The standard deviation on the estimate on T_0: $\sigma = \beta / \sqrt{r}$. r is the total number of valid fracture tests and β depends on the relative position of the test temperatures with regard to T_0.

It is clear that the C(T) specimen geometry results in the highest, i.e. most conservative, estimate for the material's transition temperature T_0. Both deep crack bend configurations basically lead to the same T_0 value, which is approximately 10 °C lower than the C(T) result. The latter confirms the "best estimate" average difference put forward in [1]. Finally, it must be noted that the use of shallow crack bend bars gives raise to a drastic drop of T_0 (52 °C with respect to the C(T) value).

RT_{T0} = T_0 + 19.4 °C was evaluated for the C(T) specimen fracture experiments (resulting in -75.4 °C) and the corresponding ASME K_{Ic} curve was plotted together with the standard ASTM MC: see Figure 8. From this graph it is again apparent that the RT_{T0}-based K_{Ic} curve is clearly situated below the MC 5% lower bound, confirming the high degree of conservatism associated with the ASME approach.

5. ANALYSES USING SELECTED CONSTRAINT-BASED METHODOLOGIES

5.1. Evaluation and estimated impact of T_{stress}

T_{stress} was calculated for each experiment using handbook formulas given in [19]. For all tested bend bars, following equation was used:

$$\frac{T_{stress}}{\sigma} = -0.630 + 1.448\left(\frac{a}{W}\right) + 4.042\left(\frac{a}{W}\right)^2 - 18.006\left(\frac{a}{W}\right)^3 + 22.289\left(\frac{a}{W}\right)^4 \qquad \text{(u)}$$

with $\sigma = 3SP/2tW^2$ (P is the load at failure, S the span, t the thickness and W the width of the bar)

For the C(T) specimens, T_{stress} was calculated as follows:

$$\frac{T_{stress}}{\sigma} = 6.063 - 78.987\left(\frac{a}{W}\right) + 380.46\left(\frac{a}{W}\right)^2 - 661.79\left(\frac{a}{W}\right)^3 + 428.45\left(\frac{a}{W}\right)^4 \qquad \text{(v)}$$

with $\sigma = P/Wt$ (P is the load at failure, W the width and t the thickness of the specimen)

The average T_{stress} values obtained for each test series are given in Table 3, together with the corresponding T_0 figures. The difference in T_{stress} between the reference SSY C(T) geometry (type A) and the type B SEN(B) configuration is obvious. T_{stress} related to specimen type C (deep notch 10x10 mm bar) is relatively high compared to the value obtained for specimen type B (deep notch 10x20 mm bar). This is basically due to the pre-fatigue cracks of the type C bars, which were generally too deep (0.56W in average). The negative T_{stress} found for the shallow notch type D bars confirms the massive loss of constraint associated with this particular geometry.

Equations (f) and (g) were checked with respect to the T_0 shift associated with the shallow notch type D bars, as compared to the deep notch type C specimens. It is clear that the found estimates (-29 °C and -16 °C, respectively) substantially underestimate the measured value: -43 °C. In order to "validate" equation (h), all available $T_0 - T_{stress}$ pairs were plotted in Figure 9. Although the number of data points is very limited, the trend predicted by (h) is largely confirmed: the relation is

basically linear and the measured slope is close to the predicted value, i.e. 1/11 instead of 1/12.

5.2. Influence of the ASTM E1921 M-factor

In paragraph 3.3. it is suggested to increase the standard M = 30 to M = 150 – 300 in order to obtain constraint-insensitive T_0 values from SEN(B) bars, more specifically from Charpy size 10x10 mm specimens. Application of this procedure (with M = 150) to the type C test series results in an invalid K_{JC} value for each single test. Hence, determination of the corresponding T_0 is not possible according to ASTM E1921. Even for the bigger type B specimens half of the test results is found to be invalid when M is set equal to 150, also hindering the determination of a valid T_0 value. Consequently this approach seems to be impracticable for constraint correction of fracture data arising from SEN(B) test programmes.

Application of formula (l) was found to be very successful to relate the outcome of the type C experiments to the reference type A tests. Individual J_c data arising from the type C 10 x 10 mm SEN(B) bars were converted into equivalent SSY C(T) values by means of this equation with M = 30. The new J_c values were used for re-evaluation of T_0, which was found to be -41.3 °C, which is exactly the same value as he one directly measured by means of the type C C(T) specimens.

Also equations (m) and (n) were checked, i.e. for conversion of 10x20 and 10x10 SEN(B) K_{Jc} data into equivalent C(T) values. In this case the calculated C(T) T_0 figures were significantly higher than the directly measured value: -31.1 °C and -29.4 °C, respectively, instead of -41.4 °C. Hence, these formulas seem to overestimate the constraint loss effects associated with BxB and Bx2B bend bars with respect to the SSY C(T) reference geometry.

5.3. Provisional evaluation of the Beremin model

Within the same CRP topic area, Weibull stress σ_w was evaluated at the IE by means of finite element analysis, both for the deep (a/W = 0.5) and shallow (a/W = 0.1) crack 10x10 SEN(B) configuration. Equation (j) was used for this purpose with a "pre-defined" m = 6 and V_0 = 1.25 10^{-4} mm^3. V corresponded to the volume where $\sigma_1 \geq 1.7\sigma_0$. Figure 10 gives the resulting $\sigma_w - J$ relation for both specimen types [20].

Although the actual calibration of the Weibull parameters σ_u and m was not carried out, the available numerical data can be used for comparing the ductile-to-brittle transition behaviour of the deep and shallow crack bend specimens. For a number of subsequent σ_w values (corresponding to "fixed but unknown" failure probabilities P_f), K_J (J) can be evaluated for both specimen types. Figure 11 shows the resulting trend. For K_J values up to 40 MPa√m, similar values are obtained for both geometries. Above 40 MPa√m obvious constraint loss is observed for the shallow

crack specimen configuration: for an arbitrary σ_w value (or failure probability P_f), the shallow crack K_J is inferior to the deep crack K_J. This trend increases towards higher failure probabilities.

The following exercise can now be made: the deep crack median MC (failure probability equal to 50%) links a K_{Jc} value of e.g. 65 MPa√m to a temperature of -88 °C. In Figure 11 a deep crack K_{Jc} of 65 MPa√m corresponds to a shallow crack K_{Jc} of 104 MPa√m. This relation is valid for any failure probability, including 50%. In other words, the Weibull approach predicts that for a shallow crack specimen tested at -88 °C, a crack-driving force of 104 MPa√m is required to reach the same failure probability of 50%. For the median deep crack MC, 104 MPa√m corresponds to a temperature of -49 °C. Consequently the shallow crack median MC will be the result of a (-88) - (-49) °C shift, i.e. -39 °C. This is very close to the MC (or T_0) shift, which was directly measured in the experimental programme: -43 °C.

6. CONCLUSIONS

The ductile-to-brittle fracture behaviour of the JRQ steel was investigated by means of four test specimen types. As expected, the C(T) specimen geometry, which corresponds to the highest crack-tip constraint conditions, resulted in the highest T_0 reference temperature (-41 °C). The standard, deeply cracked, 10x20 mm and 10x10 mm SEN(B) bars lead to comparable T_0 values: -51 °C and -52 °C, respectively. The relative loss of constraint that is traditionally associated with the 10x10 mm Charpy-size specimens, was most probably compensated by the pre-fatigue cracks, which were slightly longer than the standard maximum value. The shallow crack 10x10 mm bend specimens resulted in a large shift of T_0 down to -94 °C.

A selection of constraint-based fracture mechanics methodologies was checked against the measured T_0 variability:

- One simple linear relationship between T_0 and T_{stress} was found to be adequate for fitting all experimental data:

$$\Delta T_0 \approx \frac{T_{stress}}{12MPa/°C} \; for \; T_{stress} < 300MPa$$

- Increasing the ASTM E1921 standard *M*-factor turned out to be impracticable for constraint correction of SEN(B) fracture data. Alternatively, an exponential correction scheme, including this *M*-factor, was found to be useful for constraint correction of individual 10x10 mm *J*-integral values into equivalent C(T) data:

$$\frac{J_{SEN(B)10x10}}{J_{SSY\,C(T)}} = 1.35\left[1 + 1.5\,e^{(-M/10)}\right]$$

- In the context of the Beremin local approach method, numerically evaluated σ_w – K_{Jc} (or J) correlations were successfully used to estimate the T_0 shift connected to shallow crack 10x10 mm bend bars with respect to equivalent deeply cracked specimens.

7. REFERENCES

[1] "Standard Test Method for Determination of Reference Temperature, T_0, for Ferritic Steels in the Transition Range", ASTM Standard E 1921-05, Annual Book of ASTM Standards (Section 3, Volume 03.01), 2007

[2] N. Taylor, K. Nilsson, P. Minnebo, R. Bass, W. McAfee, P. Williams, D. Swan, D. Siegele, "An Investigation of the Transferability of Master Curve Technology to Shallow Flaws in Reactor Pressure Vessel Applications" (NESC-IV Final Report), EUR21846EN, European Commission - Joint Research Centre, 2005

[3] ASME Boiler and Pressure Vessel Code, Section III: "Rules for construction of nuclear power plant components", Subsection NB: "Division 1 Class 1 components", American Society of Mechanical Engineers, 2007

[4] ASME Boiler and Pressure Vessel Code Case N-629, "Use of Fracture Toughness Test Data to Establish Reference Temperature for Pressure Retaining Materials", Section XI, Division 1, 1999

[5] ASME Boiler and Pressure Vessel Code Case N-631, "Use of Fracture Toughness Test Data to Establish Reference Temperature for Pressure Retaining Materials other than Bolting for Class 1 Vessels", Section III, Division 1, 1999

[6] T. Anderson, "Fracture Mechanics: Fundamentals and Applications", ISBN 0-8493-4260-0, CRC Press, 1995

[7] K. Wallin, "Quantifying T_{stress} Controlled Constraint by the Master Curve Transition Temperature T_0", Engineering Fracture Mechanics 68, 303-328, 2001

[8] K. Wallin, "Structural Integrity Aspects of the Master Curve Methodology", Engineering Fracture Mechanics, 2009 – *article in press*

[9] A. Sherry, D. Hooton, D. Beardsmore, D. Lidbury, "Material Constraint Parameters for the Assessment of Shallow Defects in Structural Components. Part II: Constraint-Based Assessment of Shallow Defects", Engineering Fracture Mechanics, 72, 2396-2415, 2005

[10] F. Beremin, "A Local Criterion for Cleavage Fracture of a Nuclear Pressure Vessel Steel**",** Metallurgical Transactions, 14A, 2277-2287, 1983

[11] J. Joyce, R. Tregoning, "Development of the T_0 Reference Temperature from Precracked Charpy Specimens", Engineering Fracture Mechanics, 68, 861-894, 2001

[12] J. Heerens, R. Ainsworth, R. Moskovic, K. Wallin, “Fracture Toughness Characterisation in the Ductile-to-Brittle Transition and Upper Shelf Regimes using Pre-Cracked Single-Edge Bend Specimens”, International Journal of Pressure Vessels and Piping, 82, 649-667, 2005

[13] "Standard Test Methods for Tension Testing of Metallic Materials [Metric]", ASTM Standard E8M-04, Annual Book of ASTM Standards (Section 3, Volume 03.01), 2007

[14] “Reference Manual on the IAEA JRQ Correlation Monitor Steel for Irradiation Damage Studies”, IAEA-TECDOC-1230, International Atomic Energy Agency, 2001

[15] “Application of Surveillance Programme Results to Reactor Pressure Vessel Integrity Assessment”, IAEA-TECDOC-1435, International Atomic Energy Agency, 2005

[16] M. Scibetta, ”Procedure for shallow crack testing within the CRP8 topic area 1” (internal CRP-8 document), 2006

[17] T. Mager ed., “Reference Fracture Toughness Procedures applied to Pressure Vessel Materials”, American Society of Mechanical Engineers, 1984

[18] B. Wasiluk, J. Petti, R. Dodds, "Constraint Differences between C(T) and SE(B) for the Euro-Material", ASTM E08.08.03 Meeting, Salt Lake City, 2004

[19] A. Sherry, C. France, M. Goldthorpe, "Compendium of T-Stress Solutions for Two and Three dimensional Cracked Geometries", Fatigue and Fracture of Engineering Materials and Structures, 18, 141-155, 1995

[20] E. Paffumi, "Specification and Results for Finite Element Round Robin Part 2, Revision 2", NSU/EP/200706104F, European Commission, Institute for Energy, 2007

8. TABLES

Table 1: Nominal chemical analysis (mass %) of the JRQ Plate B test material [15].

C	Si	Mn	P	S	Cu	Ni	Cr	Mo	V
0.20	0.25	1.41	0.019	0.004	0.14	0.84	0.12	0.50	0.003

Table 2: Results from application of the ASTM E1921 procedure on the four test series data sets.

Specimen type		Average dimensions (mm)			Average	T_0 (°C)	$\Sigma r_i n_i$	σ (°C)
		W	*B*	B_{net}	*a/W*			
A	C(T)	20.0	9.9	7.9	0.53	**-41.4**	1.1	6.8
B	SEN(B)	20.0	9.9	7.9	0.52	**-50.6**	1.1	6.8
C	SEN(B)	10.0	9.9	7.9	0.56*	**-51.8**	1.1	7.1
D	SEN(B)	10.0	9.9	7.9	0.15**	**-93.7**	1.2	6.8

* outside ASTM E1921 range (0.45 – 0.55)

** non-standard ratio

Table 3: T_{stress} – evaluated from (u) and (v) – together with the corresponding T_0 value for each fracture test series.

Specimen type		T_{stress} (MPa)	T_0 (℃)
A	C(T) 10 mm a/W = 0.5	298.0	-41.4
B	SEN(B) 10x20 mm a/W = 0.5	73.2	-50.6
C	SEN(B) 10x10 mm a/W = 0.5	100.2	-51.8
D	SEN(B) 10x10 mm a/W = 0.1	-286,8	-93.7

10. FIGURES

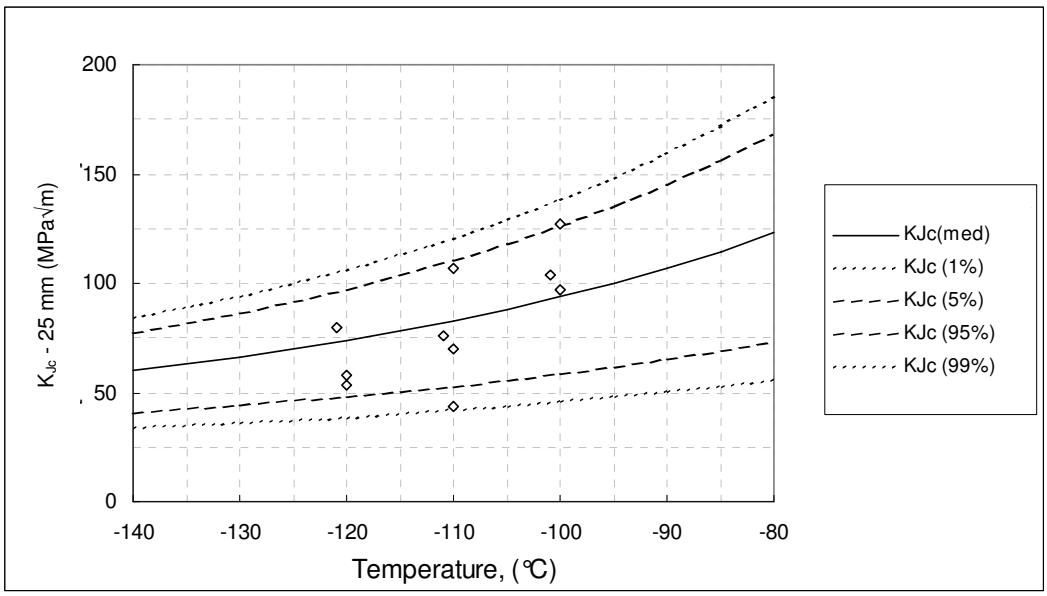

Figure 1: Fracture toughness data and MC fit for NESC-IV weld material, from tests on deeply cracked SEN(B) specimens; T_0 = -94.8 ℃ [2].

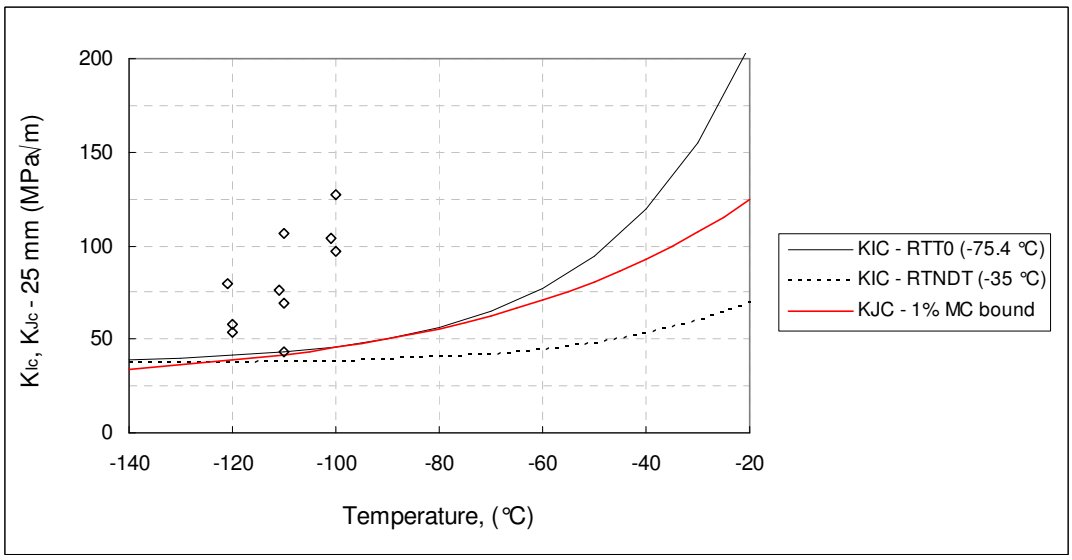

Figure 2: NESC-IV weld fracture toughness data together with the related transition curves based on the ASME RT_{To} and RT_{NDT} parameters as well as the MC 1% probability lower bound [2].

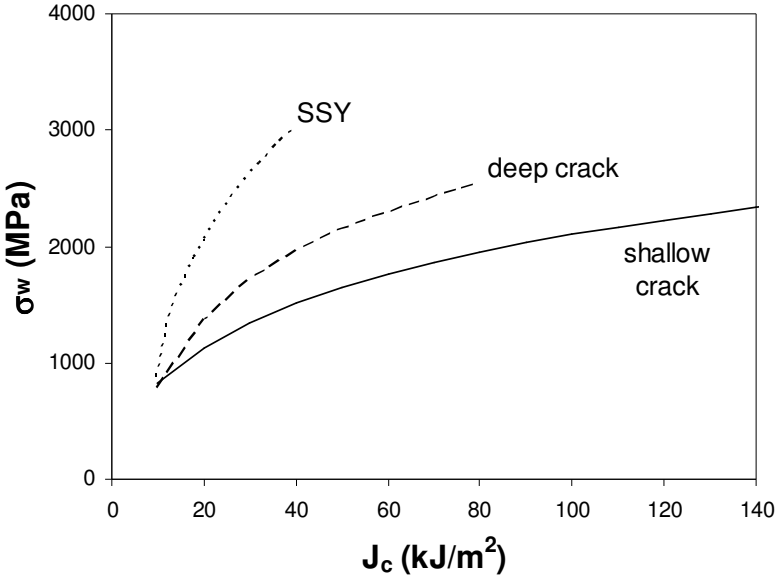

Figure 3: Schematic example of a σ_w - J relationship corresponding to the SSY situation and two selected constraint levels, e.g. a deep crack and a shallow crack SEN(B) specimen.

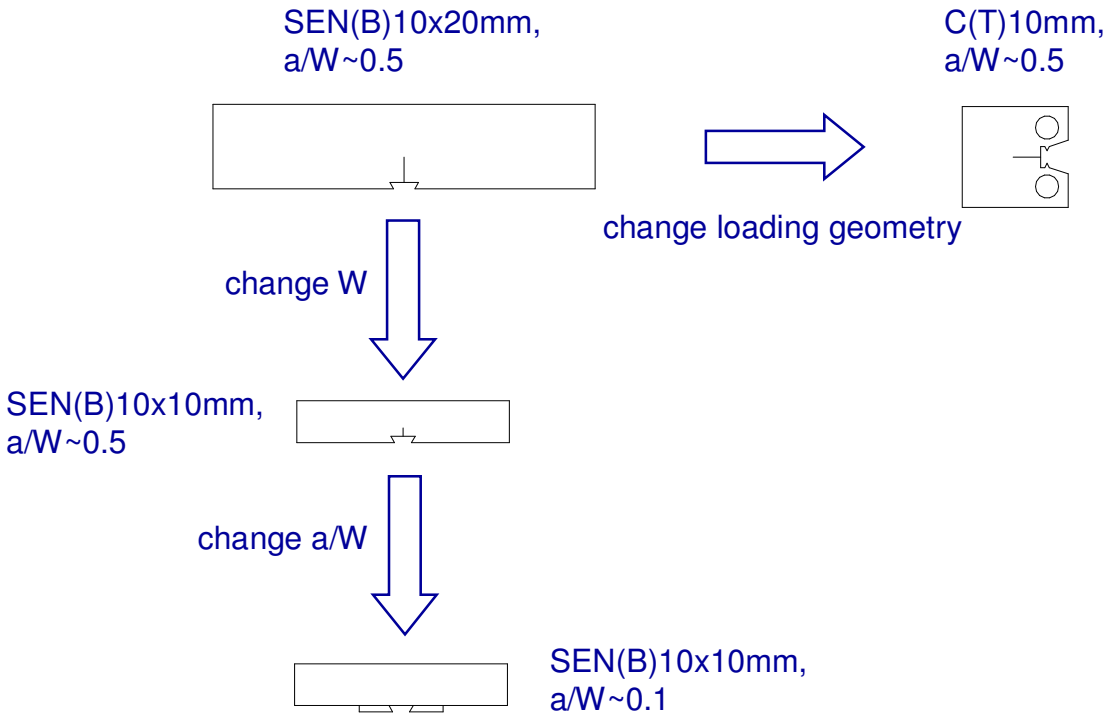

Figure 4: Schematic overview of the used laboratory specimens.

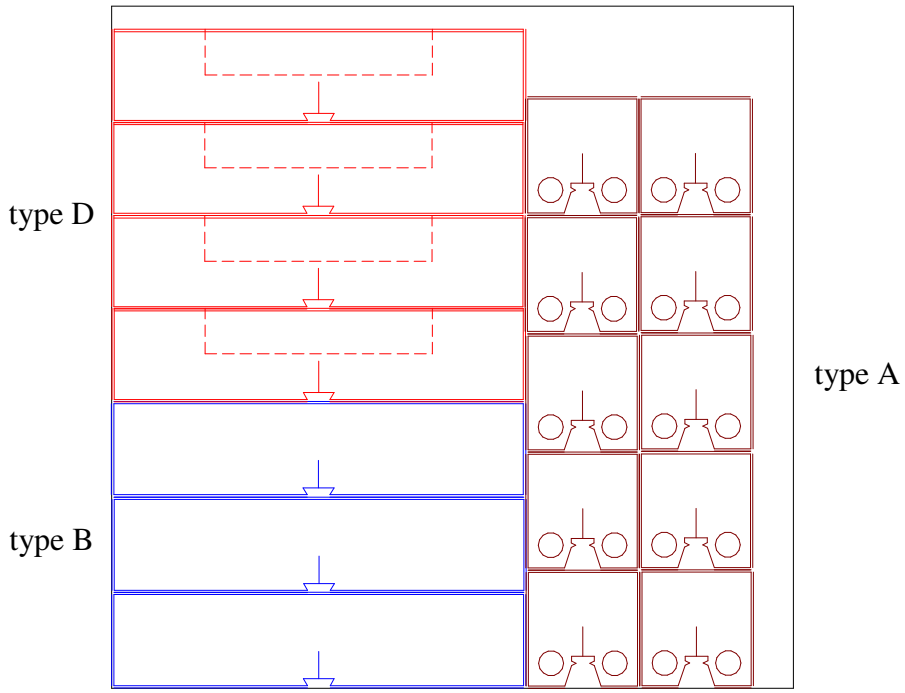

Figure 5: Part of the test specimen sampling plan.

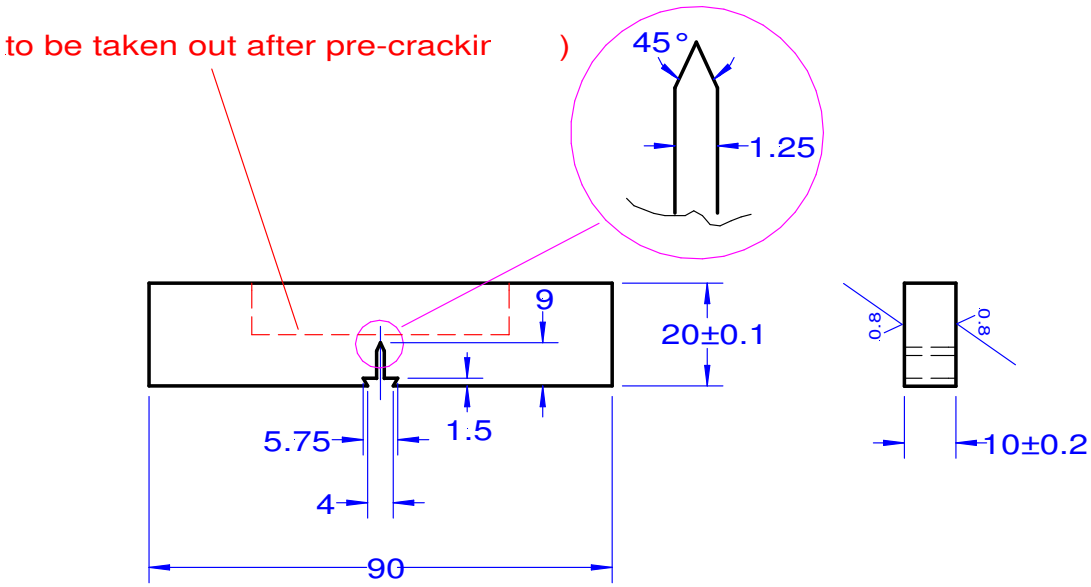

Figure 6: 10 x 20 mm type B-like bend bar to be pre-cracked and subsequently machined to the final dimensions of the type D specimen, including a 1 mm deep crack.

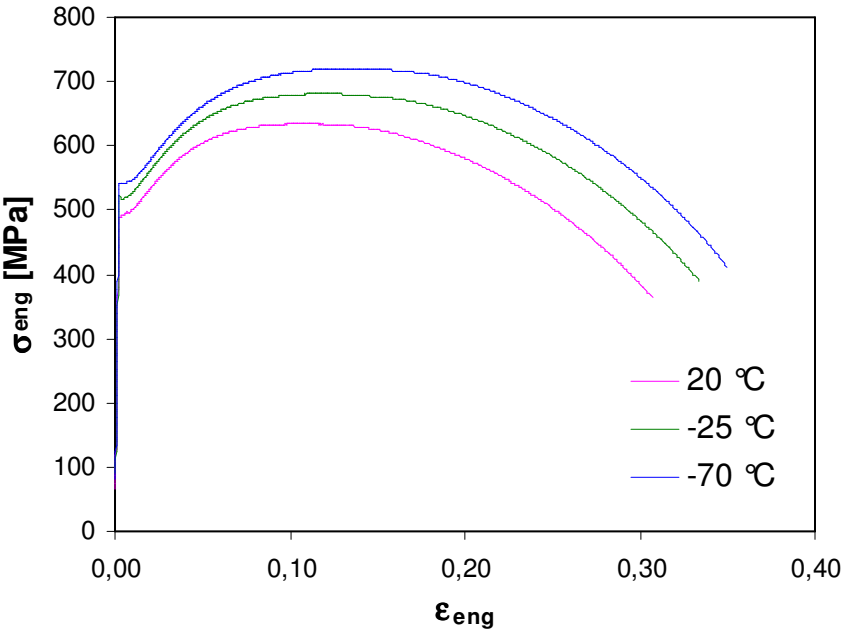

Figure 7: "8JRQ44" engineering tensile curves obtained at 20 ℃, -25 ℃ and -70 ℃.

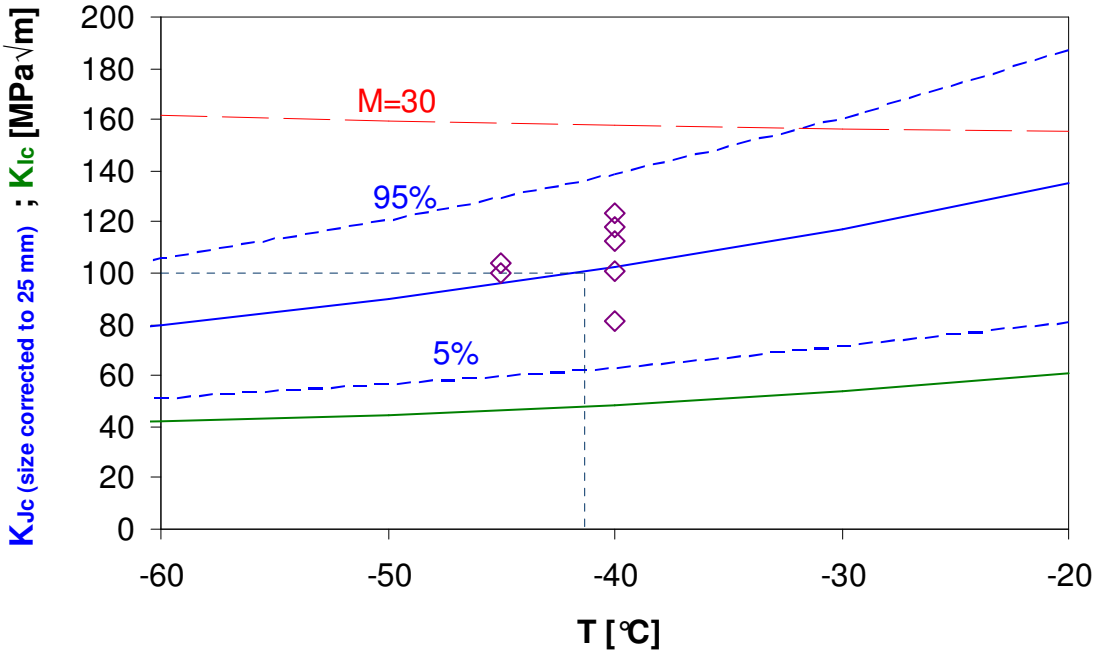

Figure 8: C(T) specimen MC (blue lines) together with the ASME K_{IC} curve based on RT_{T0} (green line).

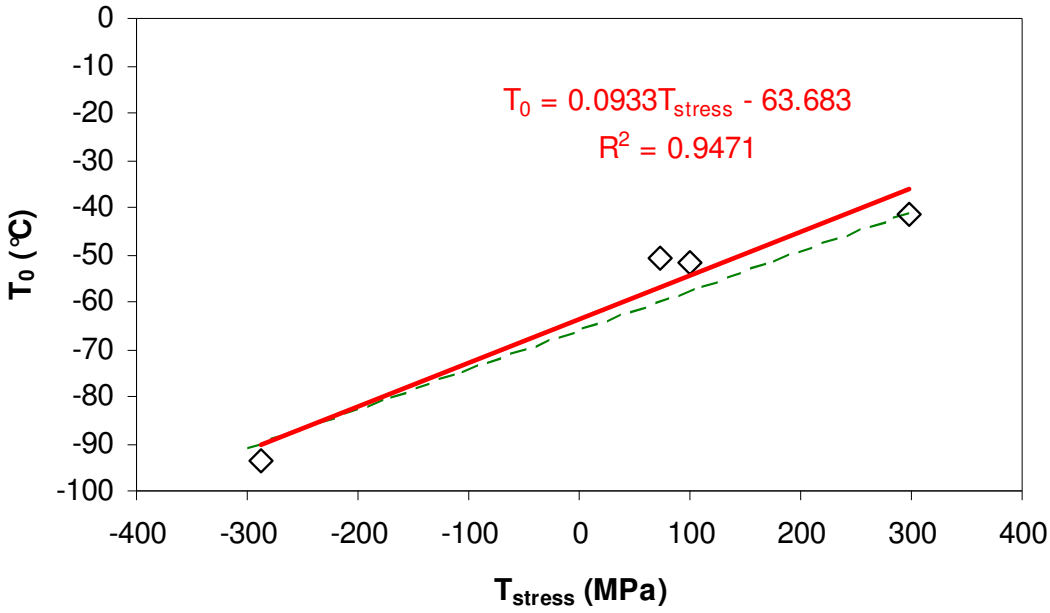

Figure 9: T_0 - T_{stress} relation arising from the four test series, red full line with slope ~1/11, together with the trend predicted by (h), green dashed line with slope 1/12.

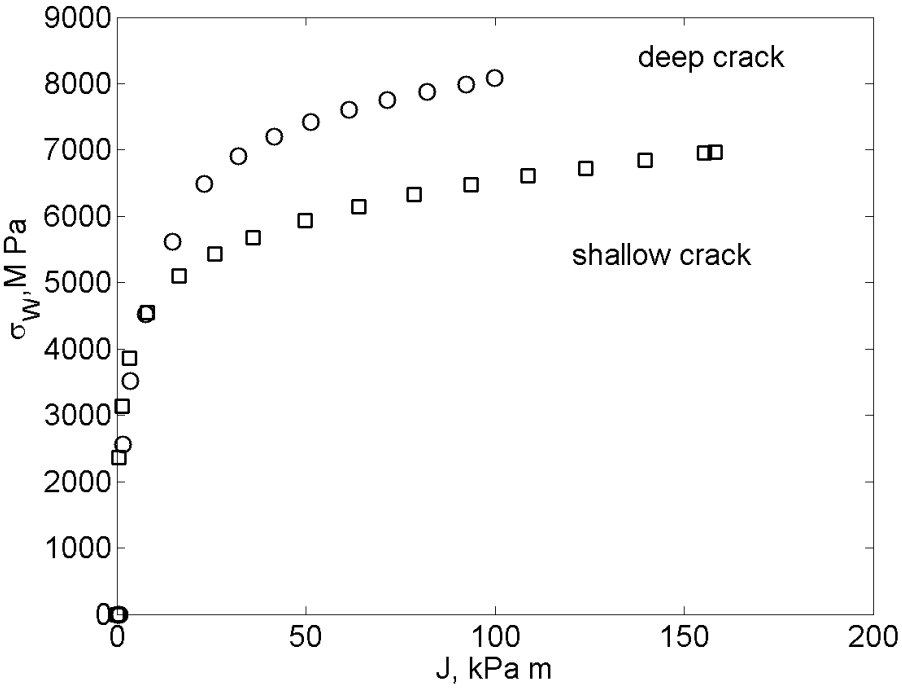

Figure 10: Weibull stress vs. *J*-integral
for deep and shallow crack 10x10 SEN(B) bars [20].

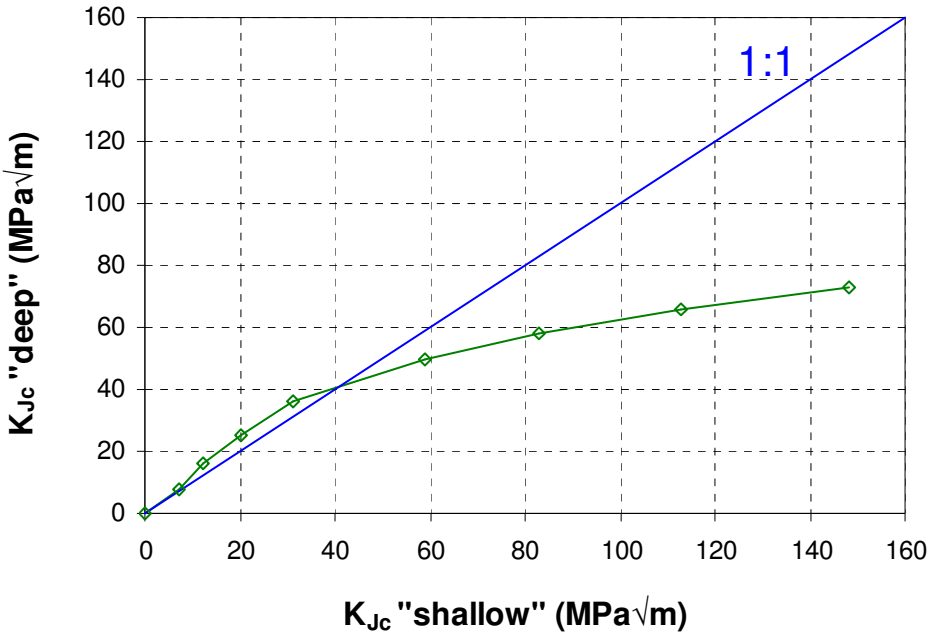

Figure 11: Equivalent K_{Jc} data for deep and shallow crack 10x10 mm bend bars, corresponding to selected Weibull stress values.

European Commission

Joint Research Centre – Institute for Energy
Title: Constraint-Based Master Curve Analysis of a Nuclear Reactor Pressure Vessel Steel
Author(s): Philip Minnebo, César Chenel Ramos, José Mendes, Luigi Debarberis

Abstract

This report presents the outcome of four fracture test series, addressing the ductile-to-brittle toughness behaviour of a nuclear reactor pressure vessel steel. Each test series corresponds to a specific test specimen geometry, tensile or three-point-bend, with a given degree of crack-tip constraint. A brief overview is given of available constraint-based fracture mechanics methodologies in the ductile-to-brittle transition range, including both engineering and local approach procedures. The obtained experimental data are analysed by means of the Master Curve standard ASTM E1921. Variability of the resulting reference temperature, T_0, is successfully confirmed by a selection of constraint-based methodologies.

The mission of the JRC is to provide customer-driven scientific and technical support for the conception, development, implementation and monitoring of EU policies. As a service of the European Commission, the JRC functions as a reference centre of science and technology for the Union. Close to the policy-making process, it serves the common interest of the Member States, while being independent of special interests, whether private or national.